Steel Plate Coupled Behavior of MEMS Transducers Developed for Acoustic Emission Testing

Didem Ozevin[a*], David W. Greve [b], Irving J. Oppenheim[c], Stephen Pessiki[a]
[a]Dept. of Civil and Environmental Engineering, Lehigh University, Bethlehem, PA 18015
[b]Dept. of Electrical and Computer Engineering, Carnegie Mellon University, Pittsburgh, PA 15213
[c]Dept. of Civil and Environmental Engineering, Carnegie Mellon University, Pittsburgh, PA 15213

Multiple narrow-band MEMS transducers located on a single chip, which are sensitive to normal surface displacement, had been developed and characterized earlier for acoustic emission testing. The chip includes 18 separate transducers tuned to frequencies between 100 kHz and 1 MHz. The MEMS chip was mounted on a steel plate excited by pencil break with two experiment configurations. In the first experiment, a single chip was used and excited from four different locations. Arrival times were computed by a threshold technique and by time-frequency graphs obtained by wavelet transform. Then, flexural wave velocities corresponding to each device frequency were computed by averaging the results of four consecutive triggers. In the second experiment, three chips were mounted on the steel plate and excited from four different locations. Source locations were determined by using wave velocities computed in the first experiment. Four transducer outputs were collected simultaneously using a multi-channel oscilloscope during both experiments. In this paper, the performance of the MEMS chip coupled to steel plate is evaluated under the consequences of these experiments. New prospects on the source location determination that are gained by the developed MEMS chip are discussed.

Keywords: Acoustic emission, MEMS, pencil break, steel plate, source location.

1. Introduction

The most promising feature of acoustic emission technology is to localize the source during a single experiment scheme. On the other hand, errors on the source location, mainly because of ambiguous solutions due to double intersections of hyperbolae, weak acoustic emission source, transducer positions, dispersion and time-difference measurement, leads to the susceptibility to the results [1]. There are several studies in the literature on the source location identification methods in order to increase the accuracy. Kosel et al. developed an intelligent acoustic emission locator [2]. Gaul and Hurleaus [3] developed a method for the source location identification at the plate by using the wavelet transform, which was developed by Kishimoto et al. [4] for beams. Holland et al. [5] showed the determination of plate source-detector separation from one signal using complete waveform recorded by a broadband transducer. This method has difficulties at near field sources and more complicated test environments as it might not be possible to separate plate modes due to multiple reflections. The method for source localization should be capable in the complex acoustical paths. Broadband type transducers were mostly used in these researches in order to capture all modes. In this study, the MEMS chip, which includes 18 independent resonant transducers tuned to frequencies in the range of 100 kHz to 1 MHz, was used to identify the source location at an isotropic plate-like structure.

* Contact author:dio2@lehigh.edu; 610-758-6966; 117 ATLSS Drive Lehigh University, Department of Civil and Environmental Engineering, Bethlehem, PA, 18015.

The MEMS chip was designed and characterized earlier [6]. Figure 1 shows the chip layout. There are two mechanical configurations called hexagon design and piston design. Hexagon designs cover higher frequencies between 350 kHz and 1 MHz and make diaphragm motion under excitation. Piston designs were designed to cover low frequencies between 100 kHz and 350 kHz and make rigid body motions under excitation at rotational and translational directions. Figure 2 shows single transducer elements and their idealization.

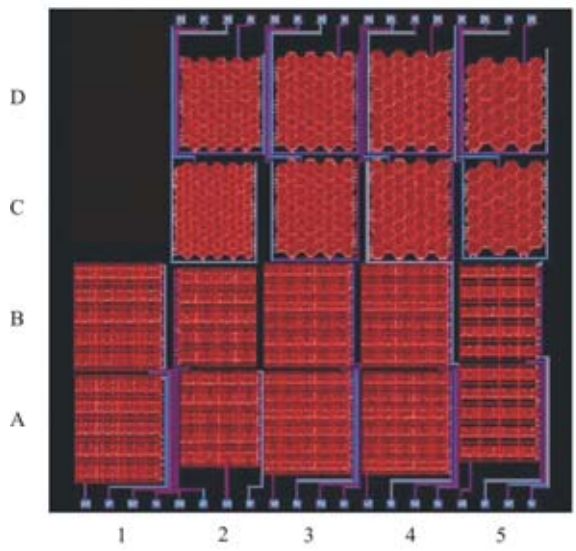

Type	Location	Resonant frequency (kHz)	
		Rotational	Translational
piston	A1	112	165
	B1	112	165
	A2	152	225
	B2	152	225
	A3	195	294
	B3	195	294
	A4	211	325
	B4	211	325
	A5	133	201
	B5	133	201
hexagon	C2	-	1065
	D2	-	812
	C3	-	660
	D3	-	660
	C4	-	482
	D4	-	482
	C5	-	362
	D5		362

Figure 1 The MEMS chip layout and transducers modal frequencies

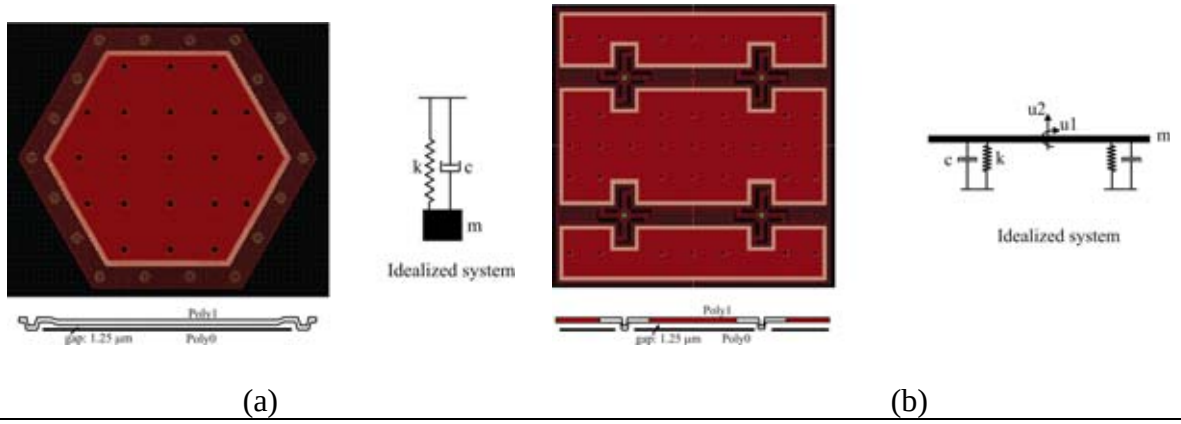

Figure 2 (a) Single hexagon unit and the idealized system, (b) single piston unit and the idealized system

2. Block Diagrams

2.1. Experiment with single chip

Experiment setup consists of 0.25cm thickness steel plate with 70X60cm^2 area as shown in Figure 3. The MEMS chip with its package and four identical amplifiers were placed on a breadboard along with a custom-designed preamplifier using LM6171 high speed low power op-amps with 100 MHz gain-bandwidth product. Amplifiers had a voltage gain of 10 up to 2 MHz and an input resistance of 100 kohm. The MEMS chips were mounted in a ceramic package with an attached

pumping port so that the ambient pressure could be varied. 8V and 20V bias voltages were applied to piston designs and hexagon designs, respectively.

The transducers were excited by 0.5mm pencil lead break from four different locations; 35 cm, 30 cm, 20 cm and 10 cm. The oscilloscope recorded the outputs of three transducers of the MEMS chip simultaneously and a PZT ultrasonic transducer mounted close to the impact point was used as trigger source. The data were sampled at 4E-7 sec.

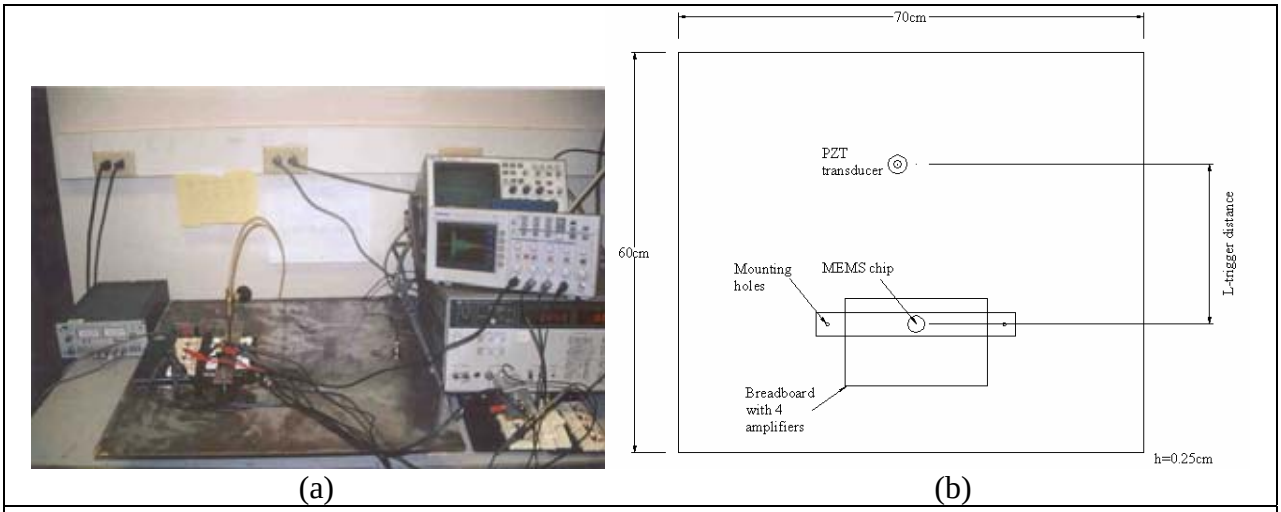

Figure 3 Steel-plate coupled experiments with a single chip (a) experiment setup, (b) experiment dimensions

2.2. Experiment with multiple chips

The test setup explained in Section 2.1 was used, but three chips were mounted on the steel plate in order to identify the source location by triangularization method. Transducers were triggered from four locations as shown in Figure 4. PZT transducer was placed closely to the excitation point and used as the trigger source. Eight different transducer sets chosen from three chips were tested.

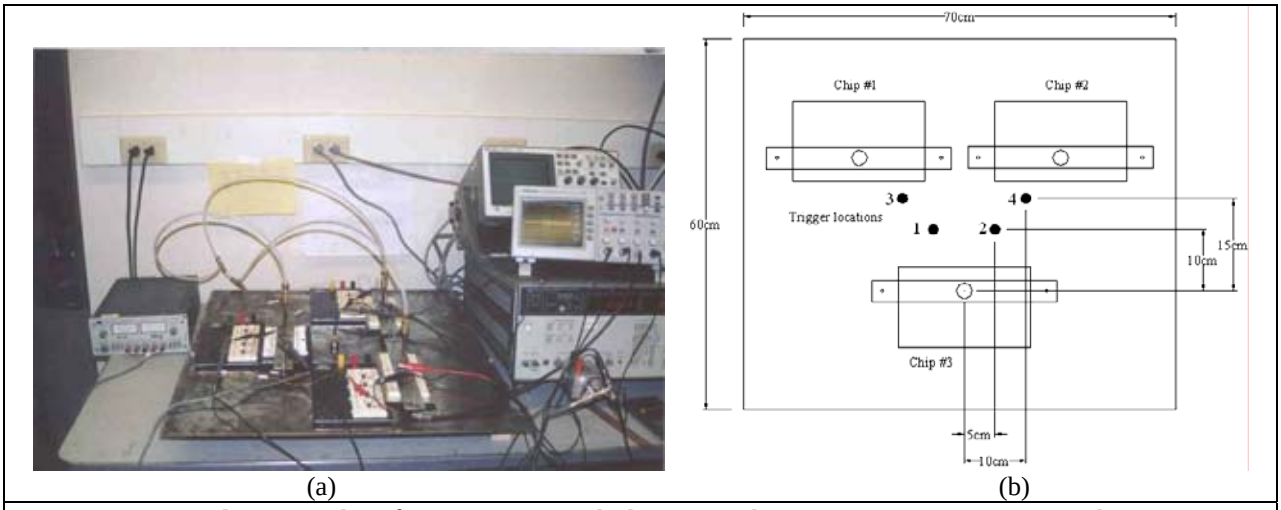

Figure 4 Source location identification setup with three transducers (a) experiment setup, (b) experiment dimensions

3. Wave Speed Computation

In this section, the group velocities of each frequency component were determined from threshold technique and time-frequency analysis. Each group in Figure 5 shows time and frequency spectra of four transducers outputs, which were recorded simultaneously and excited from a particular point. Conventional threshold technique is successful at non-dispersive environments and at dispersive environments if one particular frequency arrival is read from the time domain data. In the MEMS chip, piston type designs respond to two types of waves. Arrivals of these waveforms were separated by time-frequency analysis. Kishimoto et al. suggested using Gabor Wavelet as the Gabor function provides a small window in the time and frequency domain which augments the multiresolution of the wavelet transform and they also showed that each peak for a particular frequency corresponds to arrival of new waveform [4]. In this study, complex Morlet with the center frequency of 1.0 was chosen. Matlab wavelet toolbox was used for wavelet analyses.

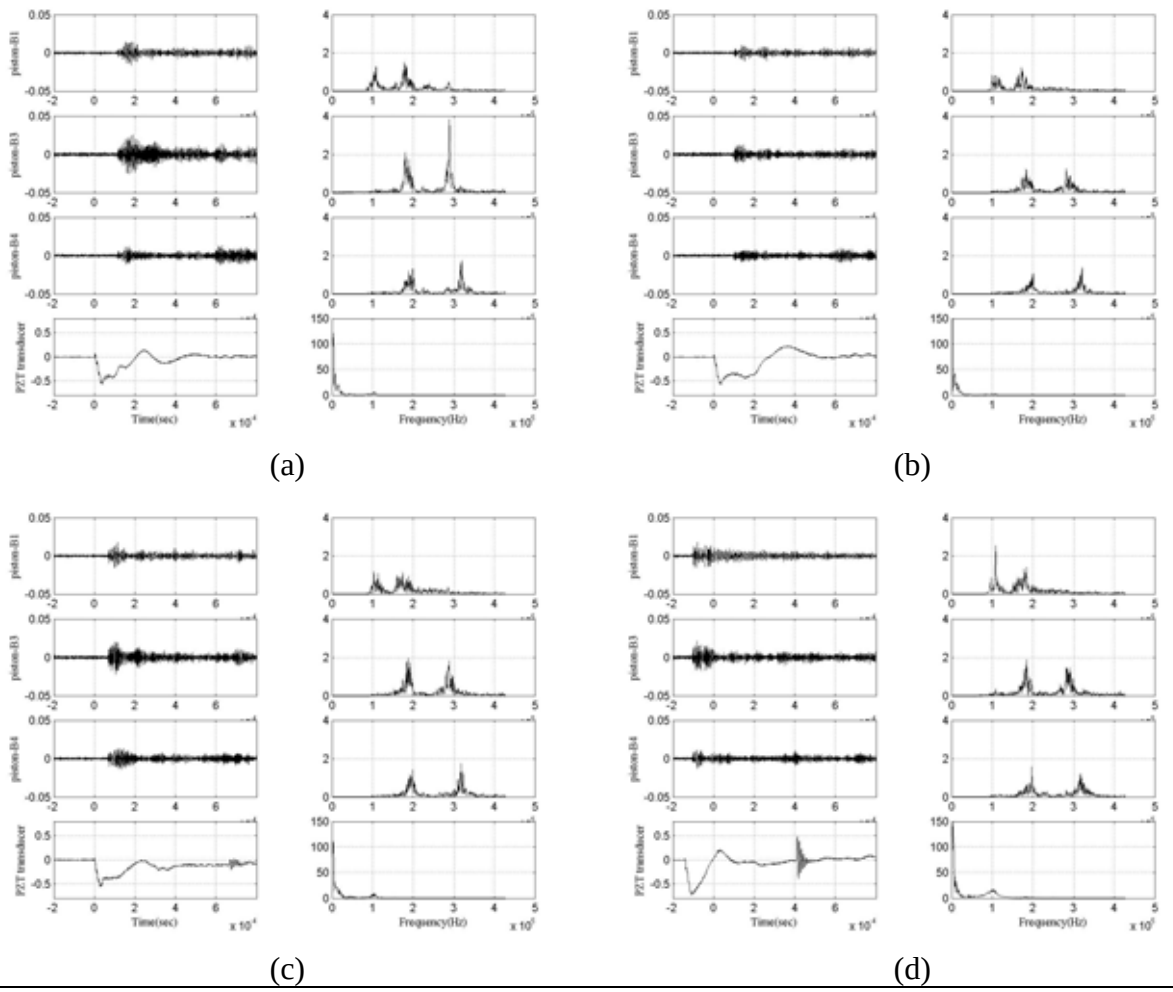

Figure 5 Time domain and frequency responses of transducer set#1 (pistons B1-B3-B4 and PZT transducer) for (a) L:35 cm, (b) L:30 cm, (c) L:20 cm, (d) L:10 cm

Figure 6 shows wavelet coefficients of signals presented at the second plots of each group in Figure 5. Scale factor represents frequency by the equation of $f = \frac{f_c}{scalefactor.\Delta}$ where f_c is the center frequency of wavelet, which is 1.0, and Δ is the sampling period, which is 4E-7 sec. Arrivals of two

resonant frequencies of piston-B3 were read from time-frequency plots, and time-distance values were plotted at Figure 7. The velocity of Lamb waves is a function of frequency and propagation mode. As the wave propagates, the different frequencies disperse and propagate at different velocities [7]. It is clear that two modes of piston designs have separate group velocities as they have different mode shapes and frequencies. The separation of two frequency components of the same acoustic emission event leads to obtain twice as much data as possible from a single transducer.

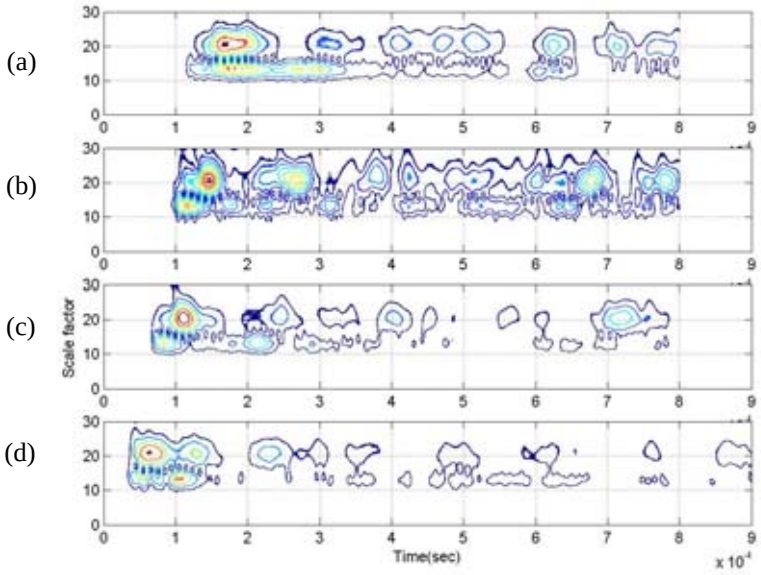

Figure 6 Wavelet coefficients of the second channel (piston-B3) of the transducer set #1 (pistons B1-B3-B4 and PZT transducer) for four different locations, (a) L:35 cm, (b)L:30 cm, (c)L:20 cm,(d)L:10 cm

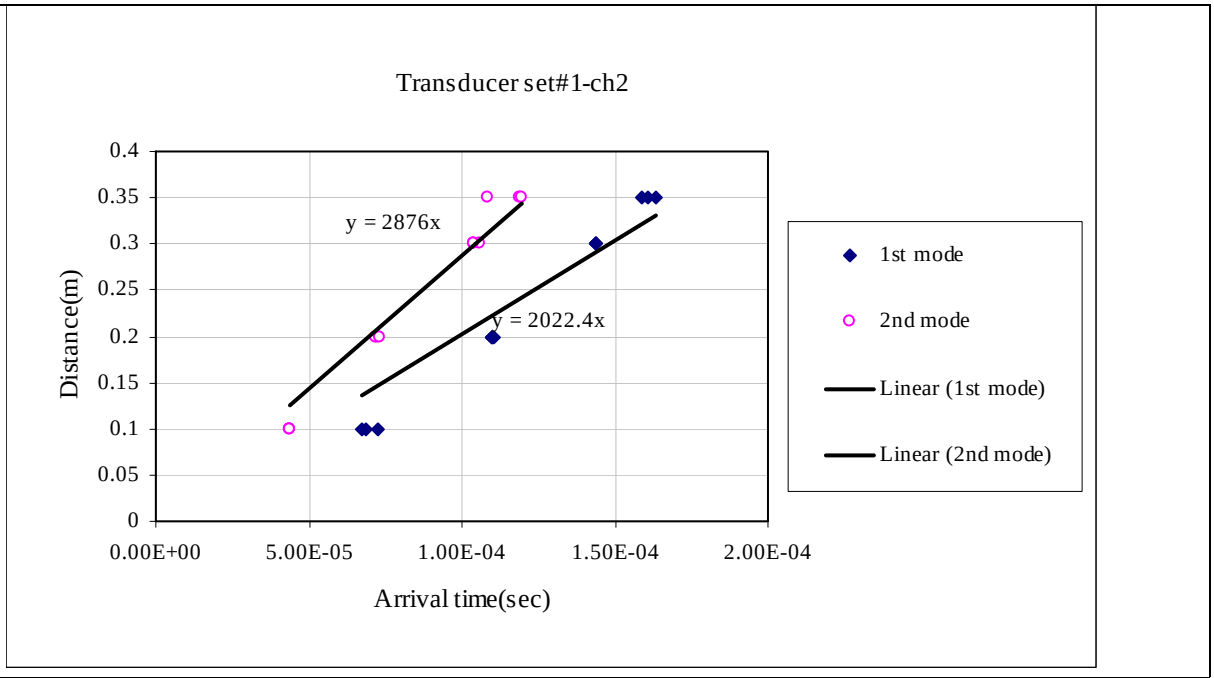

Figure 7 Velocity changes of two modes of piston designs recorded from transducer set#1 for the second channel, piston-B3

The analysis given in Figure 7 was applied to all piston type transducers. Figure 8a shows the first mode velocities of each rotational frequency. Figure 8b includes the results of both pistons and hexagons obtained from time-frequency analyses and threshold method. It is clear that threshold technique gives closer results to the fastest mode. The figure also includes the analytical result of Mindlin for the flexural waves developed by classical plate theory taking into account the shear deformation [8].

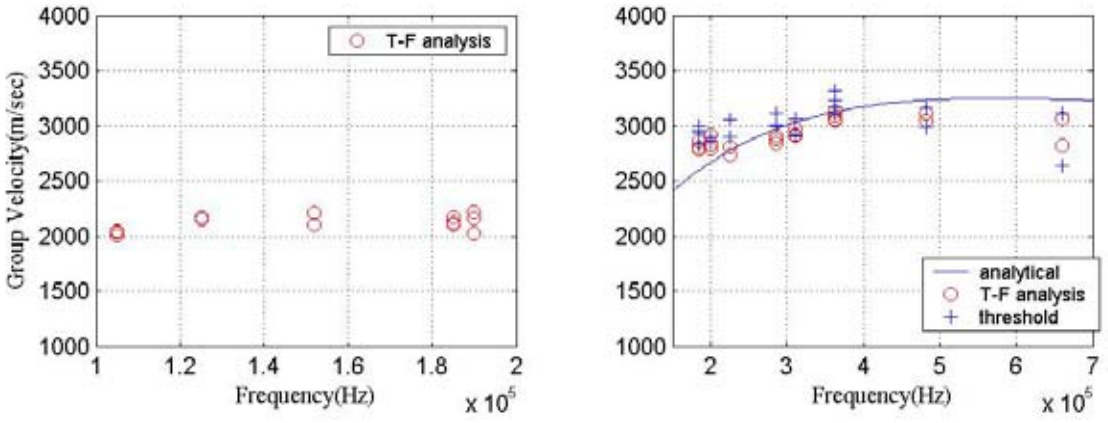

Figure 8 (a) The velocity of the rotational mode of the piston designs, (b) the velocity of the translational mode of the piston designs and hexagon designs

One of the source location errors during travel-time difference method occurs because of double intersection of the hyperbolas of two transducer pairs in region close to and behind each transducer [1]. Third hyperbole might be used, but this adds significantly to the computer processing time. The different group velocities of two piston modes help to diminish that error source. Using arrival time and velocity differences of two modes, a potential circle for the source location with the radius of $r = \Delta t.\left(\frac{1}{V_1} - \frac{1}{V_2}\right)^{-1}$ is obtained. This property reduces the error boundary.

Maji et al. suggested using two Lamb modes in order to identify the linear location of the source by filtering the signal within particular frequency range [7]. On the other hand, as there are several modes at the same frequency, error might occur if different mode was considered. However, as piston modes have distinct mode shapes and frequencies, it is easier to separate their modes and velocities.

4. Source Location Experiments

The experiment setup was explained in Section 2.2 and shown in Figure 4. Eight different transducer sets were tested under the same excitation locations. The arrival times were identified by reading from time domain data. Wave velocity was taken as 2900 m/sec for all designs as error will be small for the frequency range as shown in Figure 8b. The conventional travel-time-difference method was used to identify the source location [1]. The advantage of two piston modes was not considered here. The objective is to exploit multiple transducers located on a single chip for reducing the source location error.

In the introduction section, the main source location errors were described. It is shown above that the problem due to double intersections of hyperbolae is solved by using the two modes of piston

type designs without requiring third hyperbola. As MEMS transducers employed in this study are resonant type, weak acoustic emission source problem becomes less substantial than those of broadband transducers as the sensitivity of each particular frequency of transducers enhances with resonant behavior. Recording multiple different resonant transducer outputs located on a single chip helps to diminish time-difference measurement error as well as increase the accuracy. In addition, as the results of the same frequency transducers are compared to find the source location, the error due to velocity change with frequency disappears. Figure 9 shows the results of source identification experiments. The location of Chip#3 was taken as the origin. As there are eight data sets to compute the location, it is easy to identify the outliers if any exists in the data.

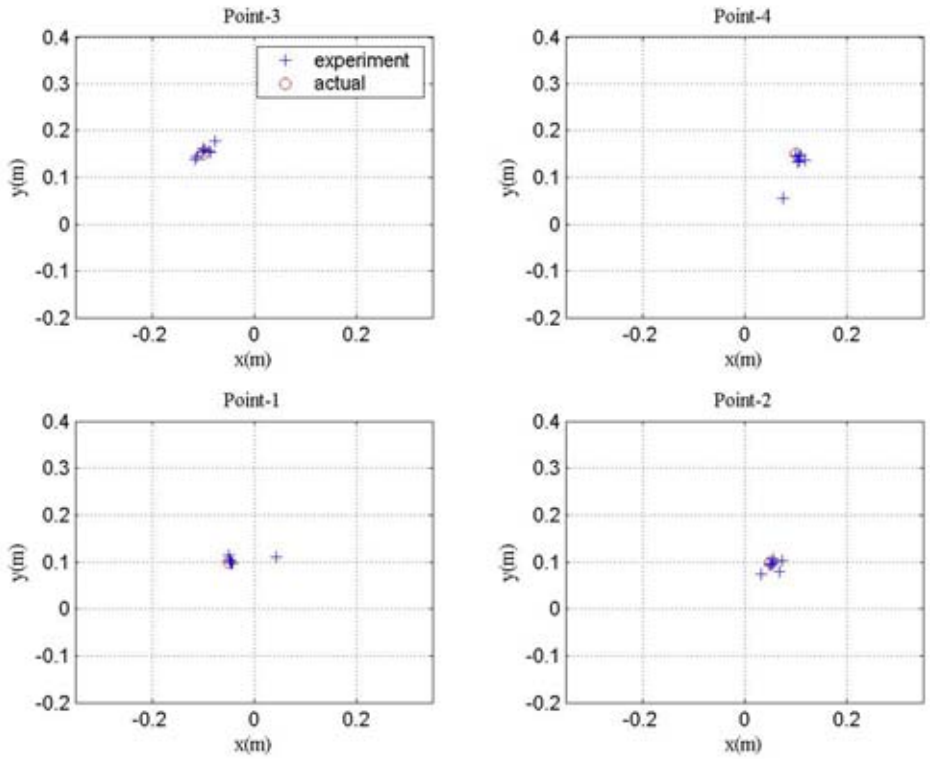

Figure 9 Source location identification using multi-channel outputs

5. Conclusion

In this study, the performance of the MEMS chip coupled to the steel plate was evaluated. It is shown that two uncoupled modes of piston type designs and the ability to record multiple resonant transducer outputs located on the same point help to diminish the source location identification errors of acoustic emission testing, which is the most promising aspect of this technology.

Acknowledgement

This material is based upon work supported by the National Science Foundation under Grant No.CMS-0329880, Pennsylvania Infrastructure Technology Alliance, and by Carnegie Mellon University and Lehigh University. The support from the sponsors is gratefully acknowledged. Any opinions, findings, and conclusions or recommendations expressed in this material are those of the authors and do not necessarily reflect the views of the sponsors.

References

1. ASTM Standard E976-00, Standard Guide for Determining the Reproducibility of Acoustic Emission Sensor Response.
2. Kosel, T., I. Grabec, F. Kosel, “Intelligent Location of Simultaneously Active Acoustic Emission Sources: Part I”, *Aircraft Engineering and Aerospace Technology*, Vol.75, 2003, p.11-17.
3. Gaul, L., S. Hurlebaus, “Identification of The Impact Location on a Plate Using Wavelets,” *Mechanical Systems and Signal Processing*, 1997, p.783-795.
4. Kishimoto, K., H. Inoue, M. Hamada, T. Shibuya, “Time Frequency Analysis of Dispersive Waves by Means of Wavelet Transform,” *Journal of Applied Mechanics*, Dec.1995, Vol.62, p.841-846.
5. Holland, S., T. Kosel, R. Weaver, W. Sachse, **“**Determination of Plate Source, Detector Separation from one Signal,” *Ultrasonics*, 2000, p.620-523.
6. Ozevin, D., S.P. Pessiki, A. Jain, D.W. Greve, I.J. Oppenheim, “Development of a MEMS Device for Acoustic Emission Testing”, *Smart Structures and Materials 2003: Smart Systems and Nondestructive Evaluation for Civil Infrastructures*, San Diego, Proc. SPIE Vol. 5057, p.64-74, March 2003.
7. Maji, A.K., D.Satpathi, T.Kratochvil, “Acoustic Emission Source Location Using Lamb Wave Modes,” *Journal of Engineering Mechanics*, Feb.1997, p.154-161.
8. Mindlin, R.D., “Influence of Rotatory Inertia and Shear on Flexural Motions of Isotropic, Elastic Plates,” *Journal of Applied Mechanics*, Vol.18, March 1951, p.31-38.